Available online at www.sciencedirect.com

Journal of Organometallic Chemistry 664 (2002) 234–244

Journal of Organometallic Chemistry

www.elsevier.com/locate/jorganchem

Steric isomerization of alkyne–dialkyltungsten complexes with a chelating diaryloxo ligand: crystal structures of C_s- and C_1-W(η^2-RC≡CR)[2,2′-S(4-Me-6-R′$C_6H_2O)_2$]$(CH_2SiMe_3)_2$

Yoshinori Takashima [a], Yuushou Nakayama [b], Hajime Yasuda [b], Akira Nakamura [c], Akira Harada [a,*]

[a] Department of Macromolecular Science, Graduate School of Science, Osaka University, 1-1 Machikaneyamachou Toyonaka, Osaka 560-0043, Japan
[b] Department of Applied Chemistry, Graduate School of Engineering, Hiroshima University, Higashi-Hiroshima 739-8527, Japan
[c] OM Research, 7-2-1308, Minami-ohgimachi, Kita-ku, Osaka 530-0052, Japan

Received 23 July 2002; received in revised form 31 August 2002; accepted 3 October 2002

Abstract

Dichlorotungsten complexes, W(η^2-EtC≡CEt)(Me_2tbp)Cl_2 (Me_2tbp = 2,2′-thiobis(4,6-dimethylphenoxo)) and W(η^2-EtC≡CEt)($^t Bu_2$tbp)Cl_2 ($^t Bu_2$tbp = 2,2′-thiobis(4-methyl-6-*tert*-butylphenoxo)) were reacted with $Mg(CH_2SiMe_3)_2$ to give the corresponding C_s-dialkyl complexes, C_s-W(η^2-EtC≡CEt)(Me_2tbp)$(CH_2SiMe_3)_2$ (**1**-C_s) and C_s-W(η^2-EtC≡CEt)($^t Bu_2$tbp)$(CH_2SiMe_3)_2$ (**2**-C_s). These C_s symmetric dialkyltungsten complexes **1**-C_s and **2**-C_s were found to undergo steric isomerization to C_1 symmetric isomers, **1**-C_1 and **2**-C_1, at 30 °C. The thermodynamic parameters for isomerization from **1**-C_s to **1**-C_1 were estimated. The structures of both the C_s- and C_1-isomers of **1** were determined by X-ray crystallography, indicating that the alkyne ligands in the C_s symmetric complexes could be regarded as four-electron donor ligands and that those in the C_1 symmetric complexes are donating two electrons. The C_1 symmetric dialkyltungsten complexes were heated to 30–60 °C to generate alkylidene species. The substituent effects of the ligands on the catalytic behavior for the ring-opening metathesis polymerization of norbornene derivatives were studied. *cis*-Contents of the poly(norbornene)s were controlled by the steric effect of alkyne and aryloxo ligands in these dialkyl complexes. The polymerization of 7-methylnorbornene catalyzed by **2**, W(η^2-PhC≡CPh)($^t Bu_2$tbp)$(CH_2Ph)_2$ (**3**-C_1) and Mo(η^2-PhC≡CPh)($^t Bu_2$tbp)Cl_2 (**5**)–$Mg(CH_2SiMe_3)_2$ gave the polymers with a *cis*-atactic structure.

Keywords: Steric isomerization; Alkyne/dialkyltungsten complexes; Crystal structures; Ring-opening metathesis polymerization

1. Introduction

Isomerization of complexes around the metal center is one of the fundamental elements in coordination chemistry and essential for understanding the mechanisms of metal-catalyzed or mediated reactions. Several isomerization reactions of octahedral molybdenum and tungsten complexes have been reported, for example, the rotational isomerization of the complexes having carbon dioxide [1], diene [2], alkyne ligands [3], and the *E*/*Z* isomerization of ketone complexes [3,4] are known. A metalla crown ether, *cis*-$Mo(CO)_4\{Ph_2P(CH_2CH_2O)_4CH_2CH_2PPh_2$-*P*,*P*′}, isomerizes in solution to yield its *trans* isomer, after photolysis of the THF solution of the *cis* isomer under a nitrogen atmosphere [5]. Complexes, *mer*-$\{MeN(C_2H_4PPh_2)_2\}M(CO)_3$ (M: Mo, W), are thermodynamically unstable and isomerize to the *fac* isomers when they are refluxed in 1,2-dichloroethane or when a trace of acid is present in their solutions [6]. However, to the best of our knowledge, structurally characterized pairs of the isomers having the same composition have not been reported in these studies.

We have reported that *cis*-dialkyltungsten complexes bearing diphenylacetylene and $^t Bu_2$tbp ligands, W(η^2-PhC≡CPh)($^t Bu_2$tbp)R_2 (R = CH_2SiMe_3, CH_2Ph, CH_3), isomerized from C_s to C_1 structure prior to α-H elimination to generate alkylidene species [7a]. In that

---

* Corresponding author. Fax: +81-6-6850-5446
E-mail address: harada@chem.sci.osaka-u.ac.jp (A. Harada).

0022-328X/02/$ - see front matter © 2002 Elsevier Science B.V. All rights reserved.
PII: S0022-328X(02)02016-8

study, only the C_1 isomers were structurally characterized. In order to get the crystal structures of the both isomers, we investigated the similar dialkyltungsten complexes having alkyne and sulfur-bridged bis(aryloxide) ligands with a variety of substituents. Here we synthesized a series of dialkyltungsten complexes coordinated with various chelating aryloxo and alkyne ligands, and got the structures of C_s–C_1 isomerizations with the same composition.

2. Results and discussion

2.1. Preparation of dialkyl complexes

A C_s dialkyltungsten complex, C_s-W(η^2-EtC≡CEt)(Me$_2$tbp)(CH$_2$SiMe$_3$)$_2$ (**1**-C_s: Me$_2$tbp = 2,2′-thiobis(4,6-dimethylphenoxo)), was prepared by the reaction of C_s-W(η^2-EtC≡CEt)(Me$_2$tbp)Cl$_2$ with Mg(CH$_2$SiMe$_3$)$_2$ (Eq. (1)). Unexpectedly, the reaction of a C_1 dichloro complex, C_1-W(η^2-EtC≡CEt)(^{t}Bu$_2$tbp)Cl$_2$, with Mg(CH$_2$SiMe$_3$)$_2$ gave a C_s complex, C_s-W(η^2-EtC≡CEt)(^{t}Bu$_2$tbp)(CH$_2$SiMe$_3$)$_2$ (**2**-C_s), at first (Eq. (1)). The corresponding C_s type dibenzyl complex, C_s-W(η^2-PhC≡CPh)(^{t}Bu$_2$tbp)(CH$_2$Ph)$_2$ (**3**-C_s), was also synthesized by using Mg(CH$_2$Ph)$_2$ instead of Mg(CH$_2$SiMe$_3$)$_2$ (Eq. (2)), which had not been isolated in our previous work [7a]. The ^{1}H-NMR spectra of these complexes **1**-C_s–**3**-C_s showed one singlet for the protons of the two *tert*-butyl or methyl substituents at 6-position, one singlet for the protons of the two methyl substituents at 4-position, and two doublets for the aromatic protons at 3- and 5-positions of the Me$_2$tbp or ^{t}Bu$_2$tbp ligand, indicating that these complexes have a C_s symmetric structure. The AB-type signals at relatively low fields (**1**-C_s: 2.48 and 1.30 ppm, $^2J_{HH} = 12.5$ Hz; **2**-C_s: 1.42 and 0.99 ppm, $^2J_{HH} = 12.3$ Hz, **3**-C_s: 3.97 and 3.26 ppm, $^2J_{HH} = 12.0$ Hz; **4**-C_s: 2.68 and 1.80 ppm, $^2J_{HH} = 12.6$ Hz) of these complexes are assignable to the α-methylene protons of W-CH_2R (R = SiMe$_3$, Ph). In their ^{13}C-NMR spectra, the alkyne carbon resonances were observed at around 249 ppm (**1**-C_s: 249.8 ppm, **2**-C_s: 249.0 ppm), which is approximate to that observed in C_s-W(η^2-PhC≡CPh)(^{t}Bu$_2$tbp)(CH$_2$SiMe$_3$)$_2$ (**4**-C_s) (244.1 ppm) [7a].

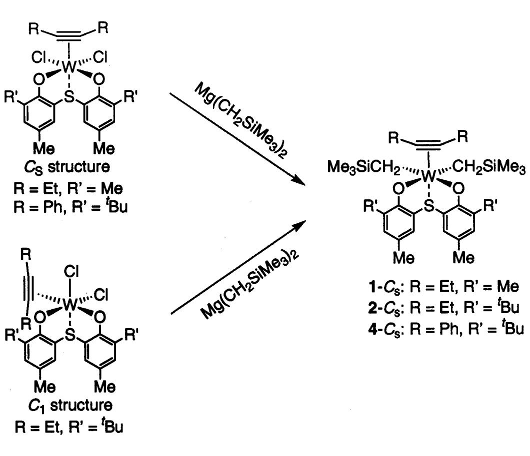

(1)

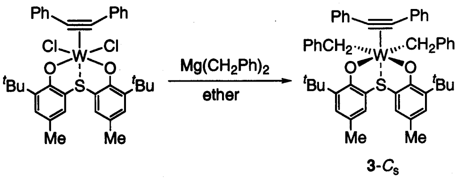

(2)

2.2. Isomerization of the dialkyl complexes

These C_s symmetric complexes **1**-C_s, **2**-C_s and **3**-C_s were found to isomerize to C_1 symmetric complexes **1**-C_1, **2**-C_1 and **3**-C_1 in C$_6$D$_6$ at 30 °C as observed for **4**-C_s [7a] (Eq. (3)). The rate of the isomerization of **1**-C_s, **2**-C_s and **3**-C_s were faster than that of **4**-C_s, the conversions of **1**-C_s and **3**-C_s were 100% after 3 h. Figs. 1 and 2 show ^{1}H-NMR spectra of complexes **1** and **3** having C_s- and C_1-structure. The 3-hexyne complexes **1**-C_1 and **2**-C_1 showed the signals for the methylene protons of one of the two trimethylsilylmethyl groups as AX-type signals at low fields (**1**-C_1: 3.77 and 2.78 ppm, $^2J_{HH} = 5.7$ Hz; **2**-C_1: 3.06 and 2.68 ppm, $^2J_{HH} = 6.5$ Hz) and those of the other trimethylsilylmethyl group were observed as AB-type signals at high fields (**1**-C_1: 1.81 and 1.53 ppm, $^2J_{HH} = 11.9$ Hz; **2**-C_1: 0.75 and 0.58 ppm, $^2J_{HH} = 12.1$ Hz). The large upfield shift of one methylene group suggests an α-H agostic interaction with the tungsten metal center in these complexes. In the ^{13}C-NMR spectrum of **1**-C_1, a resonance of alkyne carbons was observed as a single peak at 212.2 ppm due to W–alkyne free rotation. On the other hand, the diastereotopic methylene protons of one of the two alkyl groups in the diphenylacetylene complexes **3**-C_1 and **4**-C_1 were observed as AB-type signals at low fields (**3**-C_1: 5.00 and 4.72 ppm, $^2J_{HH} = 11.1$ Hz; **4**-C_1: 3.56 and 3.48 ppm, $^2J_{HH} = 7.7$ Hz) and those of the other trimethylsilylmethyl group were observed as AX-type signals at higher fields (**3**-C_1: 4.11 and 1.52 ppm, $^2J_{HH} = 10.0$ Hz; **4**-C_1: 2.33 and 0.20 ppm, $^2J_{HH} = 11.5$ Hz). In the ^{13}C-NMR spectrum, the alkyne carbon resonances were observed at 208.1 and 205.8 ppm for **3**-C_1 and at 213.9 and 210.6 ppm for **4**-C_1.

The rate of the transformation of **1**-C_s to **1**-C_1 in C$_6$D$_6$ was measured in the temperature range 30–50 °C. The decrease of **1**-C_s followed the first-order kinetic behavior as observed for **4**-C_s (Table 1), an Arrhenius plot afforded the thermodynamic data $\Delta G^\ddagger(45\ ^\circ\mathrm{C}) = 26$ kcal mol^{-1} and $\Delta S^\ddagger(45\ ^\circ\mathrm{C}) = -22$ cal K^{-1} mol^{-1}. The rate of isomerization in **2** could not be determined due to the accompanying α-H elimination, and that in **3** was

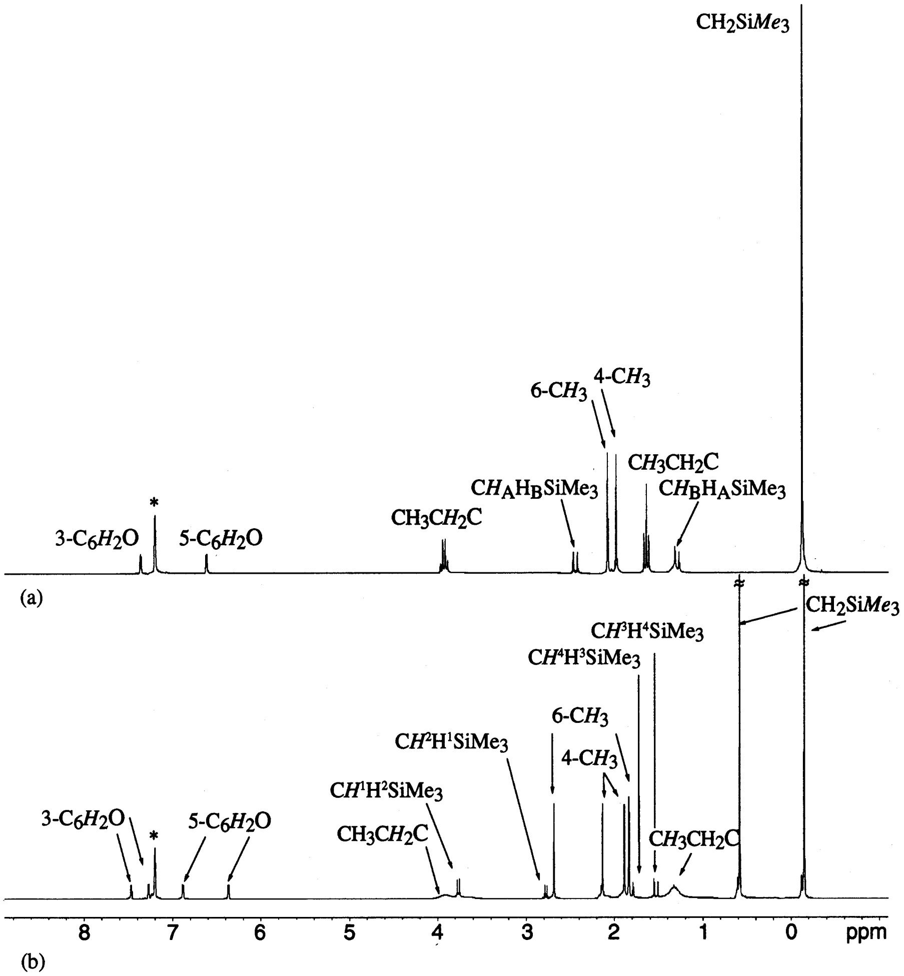

Fig. 1. ^{1}H-NMR spectra of: (a) C_s-W(η^2-EtC≡CEt)(Me$_2$tbp)(CH$_2$SiMe$_3$)$_2$ (**1**-C_s); and (b) C_1-W(η^2-EtC≡CEt)(Me$_2$tbp)(CH$_2$SiMe$_3$)$_2$ (**1**-C_1).

too fast to be monitored by ^{1}H-NMR.

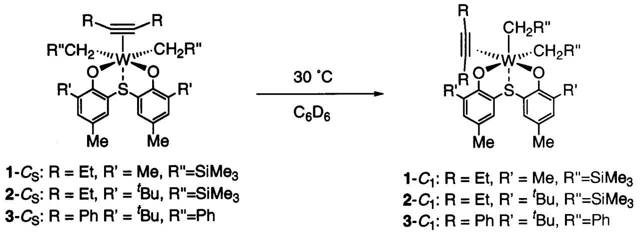

(3)

2.3. Structures of the C_s- and C_1-dialkyltungsten complexes and isomerization mechanism

We have reported about the isomerization of complex **4** and W(dpa)(^{t}Bu$_2$tbp)Cl$_2$ [7b], but we only had the structural data of the C_1 isomers. Here we got the structures of both the C_s and C_1 isomers, which enabled us to discuss the structural comparison between the C_s and C_1 isomers.

Figs. 3–5 displays the ORTEP drawings of **1**-C_s, **1**-C_1, **2**-C_s and **4**-C_s, respectively. The selected bond distances and angles of these complexes are summarized in Table 2. When the alkyne ligands are regarded to occupy one coordination site around the metal, these complexes can be best described as distorted octahedral, in which the tbp ligands coordinate to tungsten in a facial fashion. The alkyne ligands in **1**-C_s, **2**-C_s and **4**-C_s are located at the position *trans* to the sulfur atom of the tbp ligands, while that in **1**-C_1 is *trans* to the oxygen atom of the Me$_2$tbp ligand.

The W–C(alkyl) bond distance *trans* to the phenoxo moiety in **1**-C_1 (2.165(5) Å) is longer by ca. 0.042 Å than that *trans* to sulfur (2.123(5) Å) due to the *trans* influence of the phenoxo group, and is shorter by ca. 0.03 Å than those *trans* to phenoxo moiety in **1**-C_s (2.196(5) Å). This might come from the stronger coordination of the alkyne ligand to the metal center in **1**-C_s than that in **1**-C_1 (vide infra). The W–O bond distance *trans* to alkyne in **1**-C_1 (2.049(3) Å) is longer than that *trans* to trimethylsilylmethyl ligand (1.935(3) Å) due to the competitive π donation from the *trans* 3-

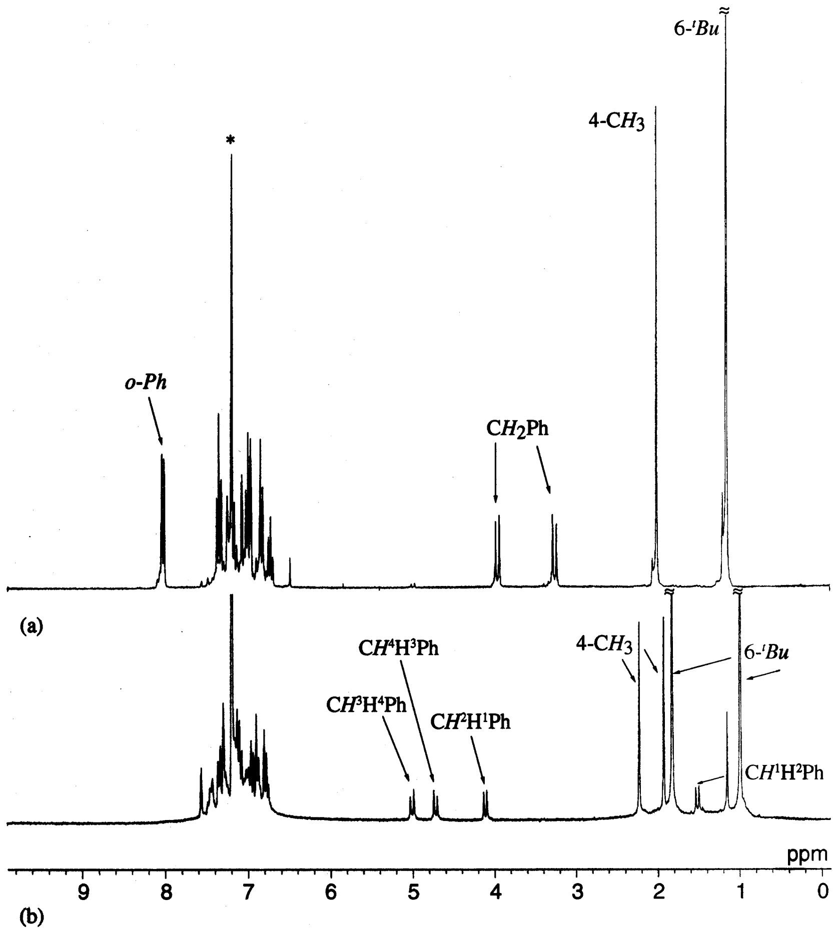

Fig. 2. ^{1}H-NMR spectra of: (a) C_s-W(η^2-PhC≡CPh)(^{t}Bu$_2$tbp)(CH$_2$Ph)$_2$ (**3**-C_s); and (b) C_1-W(η^2-PhC≡CPh)(^{t}Bu$_2$tbp)(CH$_2$Ph)$_2$ (**3**-C_1).

Table 1
Observed rate constants and half-lives at various temperatures for the isomerization of **1**-C_s to give **1**-C_1

Temperature (°C)	$10^4 k_{obs}$ (s^{-1})	$t_{1/2}$ (m)
50	10.74	10.76
45	5.28	21.88
40	3.88	29.76
35	2.19	52.77
30	1.33	86.95

hexyne ligand. The distortion of C(alkyl)–W–C(alkyl) angle from the octahedral geometry in **1**-C_1 (103.48(19)°) is significantly larger than that in **1**-C_s (87.3(3)°), while the O1–W–O2 angle in **1**-C_s (93.0(2)°) is a little deviated from the octahedral geometry as in **1**-C_1 (90.82(14)°). The W–S bond distance of **1**-C_s is similar to that of **1**-C_1.

The most notable difference between C_s and C_1 complexes is in the bonding mode of the alkyne ligands. The bond lengths and ^{13}C-NMR chemical shifts concerning the alkyne ligands in these complexes are summarized in Table 3. The W–C(alkyne) bond distances in the C_s complexes **1**-C_s, **2**-C_s, and **4**-C_s ranging from 1.997(9) to 2.027(2) Å are apparently shorter than those in the corresponding C_1 complexes, and the C≡C bond lengths of the C_s complexes also tend to be rather longer than those of the C_1 complexes. These data indicate that the alkyne ligands in the C_s complexes coordinate to tungsten more strongly than those in the C_1 complexes. In accordance with the structural data, the resonances of the alkyne carbons of the C_s complexes in ^{13}C-NMR spectra appeared at 244.5–249.8 ppm, typically for four electron donating alkynes [8–11]. In sharp contrast, the ^{13}C-NMR spectra of the C_1 complexes showed signals of the alkyne carbons at 206.7–215.4 ppm. Thus, the alkyne ligands in C_s complexes can be considered as four electron donor ligands, while those in C_1 complexes can be regarded as two electron donor ligands. Of course, these tendencies are clear in the comparison between **1**-C_s and **1**-C_1, whose compositions are completely the same. In the C_1 isomers, π-donation from the *trans* aryloxo oxygen could disturb the donation from the alkyne ligand to the same d orbitals to result in the reduced donation from the alkyne ligand. The W–O bond length *trans* to the alkyl group in **1**-C_1 (1.935(3) Å) is apparently shorter than that of **1**-C_s (1.987(4) Å), this implies that the

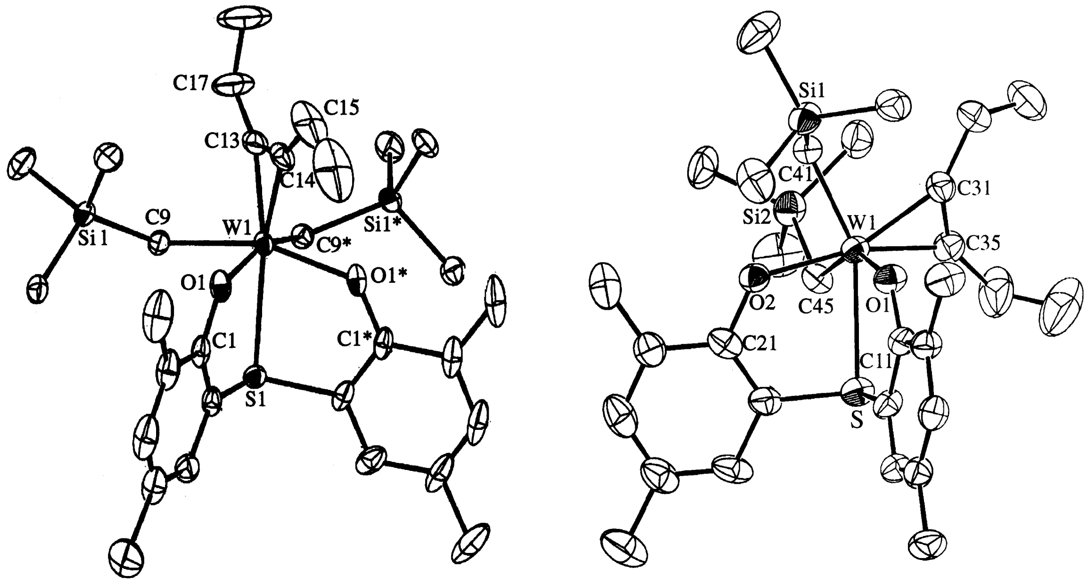

1-C_s **1**-C_1

Fig. 3. ORTEP drawing of C_s-W(η^2-EtC≡CEt)(Me_2tbp)(CH_2SiMe_3)$_2$ (**1**-C_s) and C_1-W(η^2-EtC≡CEt)(Me_2tbp)(CH_2SiMe_3)$_2$ (**1**-C_1) with a numbering scheme.

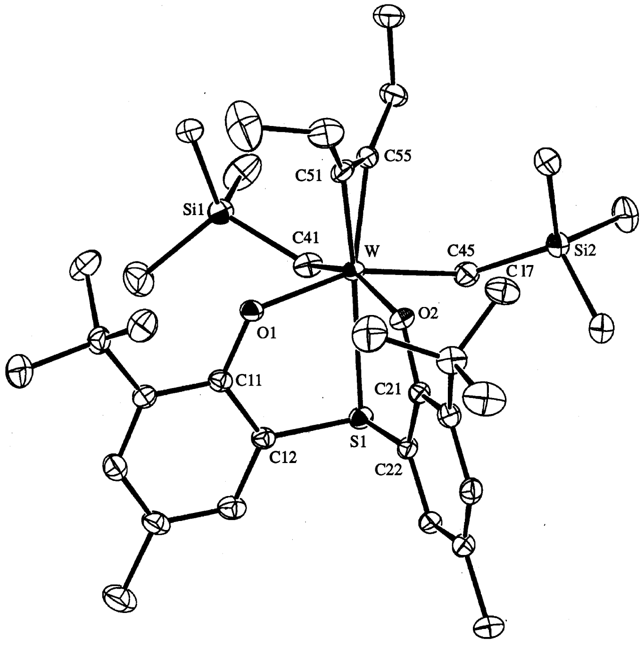

Fig. 4. ORTEP drawing of C_s-W(η^2-EtC≡CEt)(^{t}Bu$_2$tbp)(CH_2SiMe_3)$_2$ (**2**-C_s) with a numbering scheme.

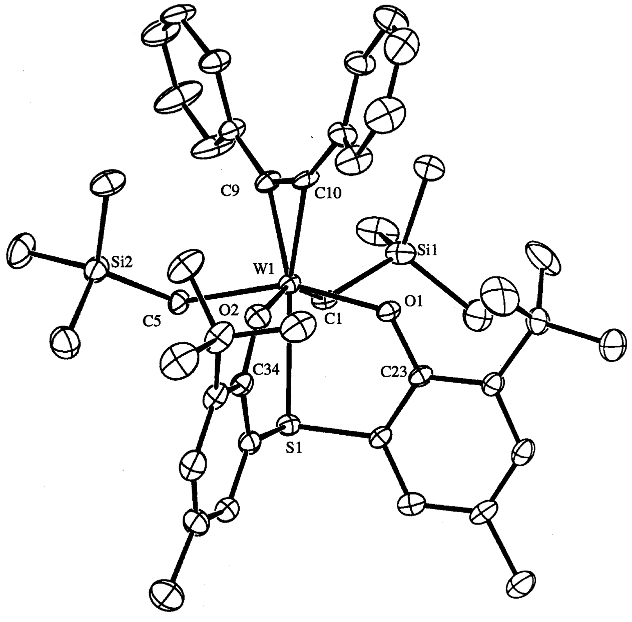

Fig. 5. ORTEP drawing of C_s-W(η^2-PhC≡CPh)(^{t}Bu$_2$tbp)(CH_2SiMe_3)$_2$ (**4**-C_s) with a numbering scheme.

electron density around the metal in **1**-C_1 is lower than that in **1**-C_s. The decreased electron density in the C_1 complexes might be one of the key elements for the subsequent α-H elimination.

We have assumed that the C_s–C_1 isomerization proceeded through a simple rotation of the two alkyl groups and one alkyne ligands around the axis through the center of those three ligands and tungsten [7a]. When the 3-hexyne complexes **1**-C_s and **2**-C_s are compared with the diphenylacetylene complex **4**-C_s, W–C(alkyne) bond distances in the **1**-C_s (av. 2.003 Å) and **2**-C_s (av. 2.012 Å) were shorter than that of **4**-C_s (av. 2.017 Å) and the W–S bond distances of **1**-C_s (2.694(3) Å) became longer than that of **4**-C_s (2.631(2) Å). We suppose that the coordination of the diphenylacetylene ligand is weaker than that of the 3-hexyne ligand, which is probably due to the delocalization of π-electrons on

Table 2
Selected bond distances (Å) and angles (°) of **1**-C_s, **1**-C_1, **2**-C_s and **4**-C_s

Complex	**1**-C_s	**1**-C_1	**2**-C_s	**4**-C_s
Bond distances				
W–O	1.987(4) (O1)	1.935(3) (O1)	1.9835(19) (O1)	1.995(4) (O1)
	–	2.049(3) (O2)	1.9905(19) (O2)	1.994(4) (O2)
W–S	2.694(3)	2.7036(13)	2.6567(7)	2.631(2)
W–C(alkyne)	1.997(9) (C13)	2.025(5) (C31)	2.013(3) (C51)	2.027(2) (C15)
	2.008(9) (C14)	2.062(5) (C35)	2.010(3) (C55)	2.007(6) (C16)
W–C(alkyl)	2.196(5) (C9)	2.123(5) (C41)	2.191(3) (C41)	2.178(7) (Cl)
	–	2.165(5) (C45)	2.184(3) (C45)	2.176(7) (C5)
C≡C(alkyne)	1.316(15)	1.278(7)	1.310(4)	1.388(8)
Bond angles				
O–W–O	93.0(2)	90.82(14)	91.39(8)	89.2(2)
C–S–C	102.1(3)	101.8(2)	102.38(13)	102.3(3)
C–W–C(alkyl)	87.3(3)	103.48(19) (alkyl)	86.04(12)	88.8(3)
W–O–C	130.3(3) (O1)	134.2(3) (O1)	130.47(18) (O1)	129.8(4) (O1)
	–	126.6(3) (O2)	130.77(17) (O2)	129.3(4) (O2)
O–W–C(alkyl)	85.50(17) (O1)	105.16(17) (O1)	85.90(10) (O1)	87.3(2) (O1)
	–	82.07(17) (O2)	87.04(10) (O2)	84.7(2) (O2)
C–W–C(alkyne)	38.4(4)	36.4(2)	38.03 (12)	38.4(2)
O–W–S	75.98(13) (O1)	73.87(10) (O1)	76.14(6) (O1)	76.1(1) (O1)
	–	75.94(10) (O2)	76.17(6)(O2)	76.9(1) (O2)
C–C≡C(alkyne)	143.0(12) (C15)	142.8(6) (C32)	142.3(3) (C52)	139.9(6) (C10)
	142.3(10) (C17)	142.9(5) (C36)	142.6(3) (C56)	141.5(6) (C17)
W–C–Si	119.5(3)	116.4(2) (Si1)	126.59(16) (Si1)	125.3(3)
	–	119.8(3) (Si2)	125.03(16) (Si2)	125.1(4)

the alkyne carbons to the phenyl rings. The distortion of O–W–O angles in **1**-C_s (93.0(2)°) and **2**-C_s (91.39(8)°) are larger than that in **4**-C_s (89.2(2)°) due to the steric hindrance of the alkyne ligand. This could be a reason for the faster isomerization rate of **1**-C_s than that of **4**-C_s.

2.4. Generation of alkylidene species from the dialkyl complexes

Further heating of these C_1 dialkyl complexes caused α-H elimination. The ^{1}H-NMR spectrum of **2**-C_1 treated at 60 °C for 24 h in C_6D_6 showed the absence of the signals for **2**-C_1 and a new signal set including the singals at 10.51 and 10.83 ppm, which could be assignable to α-H protons of alkylidene species. When **2**-C_1 was kept at room temperature in C_6D_6 for 1 month, the resonance at δ 10.51 completely disappeared and only the latter signal for the α-proton of alkylidene species was observed. The α-carbon signal of the alkylidene species appeared at 283.8 ppm in the ^{13}C-NMR spectrum. Because *anti*-isomer is generally more stable than *syn*-isomer, the signal at 10.83 ppm can be assigned to the *anti*-alkylidene species. Some other alkylidene tungsten complexes, such as W(CH–*t*-Bu)(NAr)R_2(PMe$_3$) (R = OCMe(CF$_3$)$_2$, OCMe$_2$(CF$_3$), O–*t*-Bu), W(CH–*t*-Bu)(NAr)R_2(quin) (R = OCMe(CF$_3$)$_2$, OCMe$_2$(CF$_3$)) and W(CH–*sec*-Bu)(OCH$_2$–*t*-Bu)$_3$Br have also been reported to form the alkylidene rotational isomers or rotamers [12,13]. Our efforts to isolate the alkylidene complexes have resulted in failure at present. The complex **2** was proved to be converted to alkylidene species at 30 °C for 96 h in 56% conversion by ^{1}H-NMR. When a C_6D_6 solution of **1** was heated to 60 °C in an NMR tube, the generation of an alkylidene species was not observed due to contamination by

Table 3
^{13}C-NMR and structural data concerning the alkyne ligands of the tungsten complexes

Complex	Symmetry	Chemical shift (ppm)	Distances Å (W–C)	C≡C Å
1	C_s	249.8	1.997(9), 2.008(9)	1.316(15)
1	C_1	212.2	2.025(5), 2.062(5)	1.278(7)
2	C_s	249.0	2.013(3), 2.010(3)	1.310(4)
3	C_1	208.1, 205.8	2.054(7), 2.053(7)	1.274(9)
4	C_s	244.1	2.027(2), 2.007(6)	1.388(8)
W(dpa)(^{t}Bu$_2$tbp)(CH$_3$)$_2$	C_1	208.5, 206.7	2.060(6), 2.062(7)	1.319(8)

paramagnetic byproducts. The resonances of alkyne carbons of the alkylidene species generated from **2** and **3** appears at 229.5 and 238.1 ppm, respectively, suggesting the increased electron donation from the alkyne ligands to the metal compared with those in the corresponding C_1-dialkyl complexes.

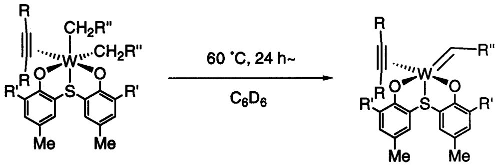

(4)

2.5. Polymerization of norbornene catalyzed by the dialkyltungsten complexes

Well-defined olefin metathesis catalysts, in particular, Group 6 alkylidene complexes having strong π-donor ligands such as imido, oxo and alkoxo have led to a precise description of the whole mechanism, and have also achieved living ring-opening metathesis polymerization (ROMP) with high selectivity [14–20]. We have reported that the complexes **3** and **4** initiated the ROMP of norbornene to give poly(norbornene) with high molecular weight and high *cis*-content [7a]. We studied here the catalytic behavior of **1** and **2** for the ROMP of norbornene to elucidate the substituent effects of the ligands on the ROMP.

The catalytic behavior of these complexes for the polymerization of norbornene was investigated in toluene, and the results are summarized in Table 4. These dialkyltungsten complexes were found to initiate the polymerization of norbornene without any cocatalysts. The use of more bulky ligands gave poly(norbornene)s with higher *cis*-contents in higher yield at 60 °C. These results agree with the previously proposed mechanism [7a] in which the steric effects of the ligands are controlling the *cis*–*trans* selectivity.

To determine the tacticity of the polymers produced by these catalysts, we investigated the polymerization of 7-methylnorbornene catalyzed by **2**, **3**, and Mo(η^2-PhC≡CPh)(^{t}Bu$_2$tbp)Cl$_2$ (**5**)–Mg(CH$_2$SiMe$_3$)$_2$ (Table 5). The ^{13}C-NMR analysis of the poly(7-methylnorbornene)s yielded a wealth of microstructural information showing diad tacticity [21]. We obtained the poly(7-methylnorbornene)s in quantitative yields with **2** and **3** catalyst system, but the yield was low in the **5**–Mg(CH$_2$SiMe$_3$)$_2$ system. All the polymers had high *cis*-contents, however, their tacticities were turned out to be completely atactic ($m = 50\%$) [21]. The higher *cis* regularity of poly(7-methylnorbornene)s than that of poly(norbornene)s can be attributed to the larger steric hindrance between the diphenylacetylene ligand and the methyl substituent of 7-methylnorbornene.

3. Conclusion

A series of tungsten complexes coordinated with various chelating aryloxo ligands and acetylene ligands, C_s-W(η^2-EtC≡CEt)(Me$_2$tbp)(CH$_2$SiMe$_3$)$_2$ (**1**-C_s, Me$_2$-tbp = 2,2′-thiobis(4,6-dimethylphenoxo)), C_s-W(η^2-EtC≡CEt)(^{t}Bu$_2$tbp)(CH$_2$SiMe$_3$)$_2$ (**2**-C_s, ^{t}Bu$_2$tbp = 2,2′-thiobis(4-methyl-6-*tert*-butylphenoxo)) and C_s-W(η^2-PhC≡CPh)(^{t}Bu$_2$tbp)(CH$_2$Ph)$_2$ (**3**-C_s), was synthesized. The bis(trimethylsilylmethyl)tungsten and dibenzyltungsten complexes isomerized from C_s- to C_1-symmetric isomers in solution and the molecular structures of both C_s and C_1 isomers of W(EtC≡CEt)(Me$_2$tbp)(CH$_2$SiMe$_3$)$_2$ (**1**) were determined by X-ray crystallography, which indicated that the alkyne ligand changed from four to two electron donor upon C_s–C_1 isomererization. The substituent effects of the ligands on the catalytic behavior of the complexes for the ROMP of norbornene derivatives were studied. In the polymerization of norbornene by these complexes, the use of more bulky ligands gave poly(norbornene)s with higher *cis*-contents. Thus the *cis*-contents of the poly(norbornene)s

Table 4
ROMP of norbornene by bis(trimethylsilylmethyl) complexes W(RC≡CR)(R$'_2$tbp)(CH$_2$SiMe$_3$)$_2$ (**1**, **2** and **4**)

	Catalyst		Temperature (°C)	Time (h)	Yield (%)	$M_n/10^4$ [b]	M_w/M_n [b]	*cis*-Content [c] (%)
	R	R′						
1	Et	^{t}Bu	60	12	24	90	1.6	68
2	Et	Me	60	12	4	15	2.4	57
4 [a]	Ph	^{t}Bu	30	1	1.6	> 200	1.7	93
4 [a]			60	1	62	49	3.4	83

In toluene, [Monomer]$_0$/[W] = 100.

[a] Ref. [10].

[b] Determined by GPC analysis in THF calibrated with standard poly(styrene)s. Theoretical M_n value is less than the experimental one [28].

[c] Microstructure of double bonds in polymer as determined by 1H-NMR spectra [21,28,29].

Table 5
ROMP of 7-methylnorbornene by using tungsten and molybdenum complexes

Catalyst	Yield (%)	$M_n/10^4$ [a]	M_w/M_n [a]	*cis*-Content (%) [b]	Tacticity *m* (%) [b]
W(EtC≡CEt)(^{t}Bu$_2$tbp)(CH$_2$SiMe$_3$)$_2$ (**2**)	100	9.8	4.3	96	50
W(PhC≡CPh)(^{t}Bu$_2$tbp)(CH$_2$Ph)$_2$ (**3**)	100	1.6	12	93	50
Mo(PhC≡CPh)(^{t}Bu$_2$tbp)Cl$_2$ (**5**)–Mg(CH$_2$SiMe$_3$)$_2$	20	25	8.9	100	50

In toluene, [Monomer]$_0$/[*W*], 100; time = 12 h.

[a] Determined by GPC analysis in THF calibrated with standard poly(styrene)s. Theoretical M_n value is less than the experimental one [28].

[b] Microstructure of the polymers as determined by 1H-NMR spectra [21,28,29].

were found to be controlled in the wide range by the design of the catalyst precursors.

4. Experimental

4.1. General procedures

All manipulations of air- and moisture-sensitive organometallic compounds were carried out by the use of standard Schlenk techniques under an Ar atmosphere. Hexane, THF, $C_6H_5CH_3$, and C_5H_{12} were dried and deoxygenated by distillation over sodium benzophenone ketyl under Ar. Dichloromethane was distilled under Ar after drying over P_2O_5. Benzene-d_6 and $C_6H_5CH_3$-d_8 were distilled from Na–K alloy and thoroughly degassed by trap-to-trap distillation before use. Dichloromethane-d_2 and $CHCl_3$-d_1 were distilled from P_2O_5. Norbornene(bicyclo[2,2,1]hept-2-ene) purchased from the Aldrich Chemical Co. was refluxed over Na and distilled prior to use. 7-Methylnorbornene [21] and dialkylmagnesium [22] were prepared according to the literature.

The ^{1}H (600, 500, 400 and 270 MHz)-, and ^{13}C (125, 100 and 67.5 MHz)- NMR spectra in C_6H_6-d_6, CH_2Cl_2-d_2, and $CHCl_3$-d_1 were measured on VARIAN-UNITY-600, JEOL JNM-LA500, JEOL JNM-GSX400 and JEOL JNM-EX270 spectrometers. Assignments for ^{1}H- and ^{13}C-NMR peaks for some complexes were aided by 2D ^{1}H–^{1}H NOESY, 2D ^{1}H–^{1}H COSY, 2D, 2D HMQC and 2D HMBC spectra. Elemental analyses were performed at Elemental Analysis Center, Faculty of Science, Osaka University. All m.p.s of the complexes were measured in sealed tubes under an Ar atmosphere and were not corrected. ESI-MS measurements were performed on a Perkin–Elmer/Sciex API III plus spectrometer. W(η^2-PhC≡CPh)[S(4-Me–6-^{t}BuC$_6$H$_2$-O)$_2$]Cl$_2$·THF [7a], W(η^2-EtC≡CEt)(Me$_2$tbp)Cl$_2$ [7a], W(η^2-EtC≡CEt)(^{t}Bu$_2$tbp)Cl$_2$ [7b], W(η^2-PhC≡CPh)(^{t}Bu$_2$tbp)(CH$_2$Ph)$_2$ (**3**-C_1) [7a], W(η^2-PhC≡CPh)(^{t}Bu$_2$-tbp)(CH$_2$SiMe$_3$)$_2$(THF) (**4**-C_s and **4**-C_1) [7a] and Mo(η^2-PhC≡CPh)(^{t}Bu$_2$tbp)Cl$_2$(THF) (**5**) [7a] were prepared according to the literature.

4.2. Preparation of *C_s-W(η^2-EtC≡CEt)[S(4,6-Me$_2$C$_6$H$_2$O)$_2$](CH$_2$SiMe$_3$)$_2$ (**1**-C_s)*

A solution of Mg(CH$_2$SiMe$_3$)$_2$ (0.34 mmol, 1.5 equivalents) in Et$_2$O was added to a solution of **2** (0.14 g, 0.23 mmol) in Et$_2$O (30 ml) via syringe at −78 °C. After stirring for 20 min, the reaction mixture was allowed to warm to ambient temperature and stirred there for 4 h. The color of the solution changed from red to orange. All volatiles were removed under reduced pressure, followed by extraction with $C_6H_5CH_3$ (25 ml) from the resulting residue. After the extract was dried in vacuo, the crude product was recrystallized from THF (1 ml) and *n*-C_5H_{12} (5 ml) at −20 °C to give W(η^2-EtC≡CEt)[S(4,6-Me$_2$C$_6$H$_2$O)$_2$](CH$_2$SiMe$_3$)$_2$ (**1**-C_s) as orange crystals in 19% yield, m.p. 168–171 °C. ^{1}H-NMR (C$_6$D$_6$, 22.5 °C, 400 MHz): δ 7.36 (d, $^4J_{HH} = 1.61$ Hz, 2H, 3-C$_6$*H*$_2$O), 6.61 (d, $^4J_{HH} = 1.92$ Hz, 2H, 5-C$_6$*H*$_2$O), 3.91 (q, 4H, C*H*$_2$CH$_3$), 2.48 (d, 2H, $^2J_{H^AH^B} = 12.5$ Hz, C*H*$_A$H$_B$Si), 2.08 (s, 6H, 6-*Me*), 1.98 (s, 6H, 4-*Me*), 1.64 (t, 6H, CH$_2$C*H*$_3$), 1.30 (d, 2H, $^2J_{H^BH^A} = 12.5$ Hz, CH$_A$*H*$_B$Si), −0.11 (s, 18H, CH$_2$Si*Me*$_3$). ^{13}C-NMR (THF-d_8, 22.5 °C, 67.5 MHz): δ 249.8 (Et*C*), 167.2 (1-*C*$_6$H$_2$O), 130.8 (6-*C*$_6$H$_2$O), 127.7 (4-*C*$_6$H$_2$O), 126.1 (3-*C*$_6$H$_2$O), 119.9 (5-*C*$_6$H$_2$O), 65.9 (*C*H$_2$SiMe$_3$), 31.6 (*C*H$_2$CH$_3$), 22.3 (6-*Me*), 20.39 (4-*Me*), 14.6 (CH$_2$*C*H$_3$), 1.1 (Si*Me*$_3$). Anal. Calc. for C$_{30}$H$_{48}$O$_2$S$_1$-Si$_2$W$_1$: C, 50.55; H, 6.79. Found: C, 50.83; H, 6.76%.

4.3. Preparation of *W(η^2-EtC≡CEt)[S(4-Me–6-^{t}BuC$_6$H$_2$O)$_2$](CH$_2$SiMe$_3$)$_2$ (**2**-C_s)*

The **2**-C_s was synthesized and isolated as orange crystals in 26% yield in a similar manner to **1**-C_s. ^{1}H-NMR (THF, 0 °C, 500 MHz): δ 7.42 (d, $^4J_{HH} = 1.65$ Hz, 2H, 3-C$_6$*H*$_2$O), 6.98 (d, $^4J_{HH} = 1.96$ Hz, 2H, 5-C$_6$*H*$_2$O), 3.99 (q, 4H, C*H*$_2$CH$_3$), 2.23 (s, 6H, 4-*Me*), 1.62 (t, 6H, CH$_2$C*H*$_3$), 1.42 (d, 2H, $^2J_{H^AH^B} = 12.2$ Hz, C*H*$_A$H$_B$Si), 1.23 (s, 18H, 6-^{t}*Bu*), 0.99 (d, 2H, $^2J_{H^BH^A} = 12.4$ Hz, C*H*$_B$H$_A$Si), −0.25 (s, 18H, CH$_2$Si*Me*$_3$). ^{13}C-NMR (THF, 0 °C, 125 MHz): δ 249.0 (Et*C*), 166.8 (1-*C*$_6$H$_2$O), 146.1 (6-*C*$_6$H$_2$O), 131.8 (4-*C*$_6$H$_2$O), 131.5 (3-*C*$_6$H$_2$O), 130.6 (5-*C*$_6$H$_2$O), 122.3 (2-*C*$_6$H$_2$O), 56.1 (*C*H$_2$SiMe$_3$), 35.7 (*C*Me$_3$), 32.9 (*C*H$_2$CH$_3$), 30.2 (C*Me*$_3$), 20.9 (4-*Me*), 15.2 (CH$_2$*C*H$_3$), 3.6 (Si*Me*$_3$).

Anal. Calc. for $C_{36}H_{60}O_2S_1Si_2W_1$: C, 54.26; H, 7.59. Found: C, 54.31; H, 7.65%. ESI-MS for *m*/*z*: 797 $[M+H]^+$.

4.4. Preparation of $W(\eta 2\text{-}PhC{\equiv}CPh)[S(4\text{-}Me\text{-}6\text{-}{}^{t}BuC_6H_2O)_2](CH_2Ph)_2$ (**3**-C_s)

This complex was synthesized and isolated in a similar manner to **1**-C_s. The yield of **3**-C_s was 20%. ^{1}H-NMR (C_6D_6, 22.5 °C, 270 MHz): δ 8.03 (d, 4H, *o*-*Ph*C), 7.35 (t, 4H, *m*-*Ph*C), 7.20 (t, 2H, *p*-*Ph*C), 7.20–7.03 (m, 6H, 3-C_6H_2O, *o*-CH_2Ph), 7.07 (t, 4H, *m*-CH_2Ph), 6.98–6.83 (m, 4H, 5-C_6H_2O+*p*-CH_2Ph), 3.97 (d, 2H, $^{2}J_{H^AH^B} = 11.8$ Hz, CH_AH_BPh), 3.26 (d, 2H, $^{2}J_{H^BH^A} = 12.2$ Hz, CH_BH_APh), 2.02 (s, 6H, 4-*Me*), 1.16 (s, 18H, 6-^{t}Bu). Anal. Calc. for $C_{50}H_{52}O_2S_1W_1$: C, 66.66; H, 5.82. Found: C, 66.60; H, 6.05%.

4.5. Isomerization of C_s-dialkyl complexes to C_1-complexes

4.5.1. Typical procedure

The complex **1**-C_s was dissolved in C_6D_6 (0.6 ml) in a 5 mm NMR tube, which was sealed under Ar and placed for a day at room temperature (r.t.). The color changed from red to pale orange, and the ^{1}H- and ^{13}C-NMR spectra of the solution were measured. **1**-C_1: ^{1}H-NMR (C_6D_6, 22.5 °C, 400 MHz): δ 7.46 (d, $^{4}J_{HH} = 2.06$ Hz, 1H, 3-C_6H_2O), 7.27 (d, $^{4}J_{HH} = 1.92$ Hz, 1H, 3′-C_6H_2O), 6.89 (d, $^{4}J_{HH} = 2.12$ Hz, 1H, 5-C_6H_2O), 6.37 (d, $^{4}J_{HH} = 1.84$ Hz, 1H, 5′-C_6H_2O), 3.92 (br, 4H, CH_2CH_3), 3.77 (d, 1H, $^{2}J_{H^1H^2} = 5.7$ Hz, CH^1H^2Si), 2.78 (d, 1H, $^{2}J_{H^2H^1} = 5.7$ Hz, CH^2H^1Si), 2.69 (s, 3H, 6-*Me*), 2.14 (s, 3H, 4-*Me*), 1.89 (s, 3H, 4′-*Me*), 1.84 (s, 3H, 6′-*Me*), 1.81 (d, 1H, $^{2}J_{H^4H^3} = 11.9$ Hz, CH^4H^3Si), 1.53 (d, 1H, $^{2}J_{H^4H^3} = 11.9$ Hz, CH^3H^4Si), 1.34 (br, 6H, CH_2CH_3), 0.57 (s, 9H, SiMe_3), −0.14 (s, 9H, SiMe'_3). ^{13}C-NMR (CD_2Cl_2, 30 °C, 150 MHz): δ 212.2 (br, Et*C*), 167.3 (4-C_6H_2O), 165.7 (4′-C_6H_2O), 133.8 (5-C_6H_2O), 133.6 (5′-C_6H_2O), 131.3 (6-C_6H_2O), 131.2 (6′-C_6H_2O), 130.9 (3-C_6H_2O), 128.8 (3′-C_6H_2O), 128.3, 126.6, 120.4, 118.9, 86.1 (CH^1H^2Si, $^{1}J_{CH^1} = 116$, $^{1}J_{CH^2} = 107$ Hz), 72.6 (CH^3H^4Si, $^{1}J_{CH} = 113$ Hz), 26.8 (br, CH_2CH_3), 20.5 (4-*Me*), 20.4 (4′-*Me*), 17.9 (6-*Me*), 17.2 (6′-*Me*), 14.8 (CH_2CH_3), 2.9 (SiMe_3), 1.2 (SiMe'_3). **2**-C_1: ^{1}H-NMR (C_6D_6, 22.5 °C, 400 MHz): δ 7.58 (d, $^{4}J_{HH} = 2.10$ Hz, 1H, 3′-C_6H_2O), 7.32 (d, $^{4}J_{HH} = 2.04$ Hz, 1H, 3-C_6H_2O), 7.24 (d, $^{4}J_{HH} = 2.11$ Hz, 1H, 5′-C_6H_2O), 6.79 (d, $^{4}J_{HH} = 2.06$ Hz, 1H, 5-C_6H_2O), 3.73 (br, 4H, CH_2CH_3), 3.06 (d, 1H, $^{2}J_{H^3H^4} = 6.47$ Hz, CH^3H^4Si), 2.68 (d, 1H, $^{2}J_{H^4H^3} = 6.50$ Hz, CH^4H^3Si), 2.20 (s, 3H, 4′-*Me*), 1.95 (s, 3H, 4-*Me*), 1.79 (s, 9H, 6-^{t}Bu), 1.29 (br, 6H, CH_2CH_3), 1.14 (s, 9H, 6′-^{t}Bu), 0.75 (d, 1H, $^{2}J_{H^2H^1} = 12.05$ Hz, CH^2H^1Si), 0.65 (s, 9H, SiMe'_3), 0.58 (d, 1H, $^{2}J_{H^1H^2} = 12.05$ Hz, CH^1H^2Si), −0.12 (s, 9H, SiMe_3). All attempts to isolate **2**-C_1 have been in failure because it was highly soluble even in C_6H_{14} at −78 °C.

4.6. Kinetic study for isomerization of **1**-C_s to **1**-C_1

The complex **1**-C_s (0.063 g, 0.071 mmol) was dissolved in C_6D_6 (4.00 ml) at r.t., and the solution (0.018 M) was divided equally among five NMR tubes. Each of them was sealed under Ar and kept at −20 °C until used. Reaction temperatures were maintained within ±0.1 °C by the JEOL JNM-EX270 temperature controller and progress of isomerization was monitored by ^{1}H-NMR. The value $[\mathbf{1}\text{-}C_s]_t$, which refers to the concentration of **1**-C_s at the reaction time *t*, was determined by the sum of intensities of areas assignable to 18 protons ($SiMe_3$) in **1**-C_s. Treatment of the data is described in the text.

4.7. Polymerization of norbornene

4.7.1. General procedures

To a solution of **2**-C_s (16.0 mg, 0.02 mmol) in $C_6H_5CH_3$ (1.0 ml) was added a solution of norbornene (100 equivalents, 2 mmol) in $C_6H_5CH_3$ (2 M, 1.0 ml) at 30 °C. After the solution was stirred at 30 or 60 °C for a prescribed period, MeOH (15 ml) was added to the resulting reddish viscous solution to precipitate a pale-yellow polymer. The polymer was washed with MeOH and then dried in vacuo.

The *cis*-content of double bond of the polymers was determined comparison of ^{1}H-NMR with that of the literature [21]. Unfortunately, the ^{13}C-NMR spectrum of poly(norbornene)s displayed no resonances for *m*/*r* splitting. In order to determine the tacticity of the polymer, we used 7-methylnorbornene as a monomer. Polymerization of a 1:1 mixture of *syn*- and *anti*-7-methylnorbornene by using **2** as a catalyst afforded poly(*anti*-7-methylnorbornene)s, whose tacticities were determined by comparison of the ^{13}C-NMR spectral data [21].

4.8. GPC analysis of the polymers

For the polymers obtained by using **2**–**4** as catalysts, Gel permeation chromatographic (GPC) analyses were carried out at 40 °C using Tosoh TSKgel HXL-H and L columns connected to a Tosoh RI-8012 detector. Samples were prepared in THF (0.1–0.3% (w/v)) and were filtered through an Advantec DISMIC-25JP filter in order to remove particulate before injection. GPC columns were calibrated versus commercially available polystyrene standards (Polymer Laboratories Ltd.) whose molecular weight ranged from 500 to 2.15×10^6.

4.9. Crystallographic data collections and structure determination of **1**-C_s, **1**-C_1, **2**-C_s and **4**-C_s

The crystals of **1**-C_s, **1**-C_1 and **2**-C_s suitable for X-ray diffraction studies were mounted on a cryoloop. The measurement of **1**-C_s, **1**-C_1 and **2**-C_s was made on a Rigaku R-AXIS-RAPID Imaging Plate diffractometer with graphite monochromated Mo–K_α radiation ($\lambda = 0.71069$). Relevant crystal and data statistics are summarized in Table 6. Indexing was performed from one oscillations which were exposed for 5.0 min. The camera radius was 127.40 mm. Read-out was performed in the 0.100 mm pixel mode. A symmetry-related absorption correction using the program ABSCOR [23] was applied. The data was corrected for Lp effects. The structures of complex **1**-C_s was solved by direct methods (SHELXS-86) [24] and expanded using Fourier techniques (DIRDIF-94) [25] and refined by full-matrix least-squares refinement (SHELXL-97) [26]. The structure of complex **1**-C_1 was solved by direct methods (SHELXS-97) [26] and expanded using Fourier techniques (DIRDIF-94) [25] and refined by full-matrix least-squares refinement (SHELXL-97) [26]. The structure of complex **2**-C_s was solved by direct methods (SIR-92) [27] and expanded using Fourier techniques (DIRDIF-94) [25] and refined by full-matrix least-squares refinement (SHELXL-97) [26]. In the subsequent refinement the function $\Sigma\ \omega(|F_o| - |F_c|)^2$ was minimized, where $|F_o|$ and $|F_c|$ are the observed and calculated structure factors amplitudes, respectively. The agreement indices are defined as $R = \Sigma\ ||F_o| - |F_c||/\Sigma\ |F_o|$ and $R_w = [\Sigma\ w(F_o^2 - F_c^2)^2/\Sigma\ w(F_o^2)^2]^{1/2}$. The positions of all non-hydrogen atoms for the complexes were found from a difference Fourier electron density maps and refined anisotoropically. All hydrogen atoms were placed in calculated positions (C–H = 0.95 Å) and kept fixed.

A crystal of **4**-C_s was sealed in a glass capillary under Ar. The crystal of **4**-C_s mounted on a Rigaku AFC-5R four-circle diffractometer for data collection using Mo–K_α radiation. Relevant crystal and data statistics are summarized in Table 6. The unit cell parameters and the orientation matrix at 23 °C were determined by a least-squares fit to 2θ values of 25 strong higher reflections for complex **4**-C_s. Three standard reflections were chosen and monitored every 150 reflections. Empirical absorption correction was carried out on the basis of an azimuthal scan. Complex **4**-C_s showed no significant intensity decay during the data collection. The structure of complex **4**-C_s was solved by direct methods (SHELXS-86) [24] and expanded using Fourier techniques (DIRDIF-94) [25] and refined by the full-matrix least-square method. Measured non-equivalent reflections with $I > 3.0\sigma(I)$ were used for the structure determination. In the subsequent refinement the function $\Sigma\ w(|F_o| - |F_c|)^2$ was minimized, where $|F_o|$ and $|F_c|$ are the observed and calculated structure factors amplitudes, respectively. The agreement indices are defined as $R = \Sigma\ ||F_o| - |F_c||/\Sigma\ |F_o|$ and $R_w = [\Sigma\ \omega(|F_o| - |F_c|)^2/\Sigma\ \omega(|F_o|)^2]^{1/2}$

Table 6
Crystal data and collection parameters of **1**-C_s, **1**-C_1, **2**-C_s and **4**-C_s

Complex	**1**-C_s	**1**-C_1	**2**-C_s	**4**-C_s
Empirical formula	$C_{30}H_{48}O_2SSi_2W$	$C_{30}H_{48}O_2SSi_2W$	$C_{36}H_{60}O_2SSi_2W$	$C_{44}H_{60}O_2SSi_2W$
Formula weight	712.77	712.77	796.93	893.04
Temperature (K)	200(2)	296(2)	193(1)	296(1)
Crystal system	Orthorhombic	Monoclinic	Monoclinic	Triclinic
Space group	*Pnma* (#62)	*C*2/*c* (#15)	*P*2$_1$/*c* (#14)	*P*$\bar{1}$ (#2)
a (Å)	12.0641(6)	35.418(2)	19.5341(4)	13.299(5)
b (Å)	22.1541(11)	10.3063(6)	16.8368(3)	14.329(7)
c (Å)	12.1829(5)	19.0312(12)	19.7103(1)	12.344(4)
α (°)	–	–	–	98.18(4)
β (°)	–	103.892(2)	143.06	110.01(3)
γ (°)	–	–	–	91.78(4)
V (Å^3)	3256.1(3)	6743.8(7)	3895.51(13)	2179(1)
Z	4	8	4	2
D_{calc} (g cm^{-3})	1.454	1.404	1.359	1.361
F(000)	1448.00	2896.00	1640.00	916.00
μ (Mo–K_α) (cm^{-1})	37.09	35.82	31.08	27.89
Scan speed (° min^{-1})	–	–	–	16.0
Scan width (°)	–	–	–	$1.63 + 0.35 \tan \theta$
$2\theta_{max}$ (°)	55.0	55.0	54.8	55.0
Unique data (R_{int})	3835	7266	8840	9983
Observations	2685	5834	6669	5991
Variables	182	337	395	467
R	0.0271	0.0366	0.0290	0.037
R_w	0.0728	0.1034	0.0524	0.038
Goodness-of-fit	1.352	1.092	0.934	1.12

where $\omega^{-1} = \sigma^2(F_o) = [\sigma_c^2(F_o) + p^2/4(F_o^2)]$. The positions of all non-hydrogen atoms for complex **5**-C_s were found from a difference Fourier electron density map and refined anisotropically. Hydrogen atoms were refined isotropically, and they were placed in calculated positions (C–H = 0.95 Å) and constrained to ride on their respective carbon atoms.

All calculations were performed using the TEXSAN crystallographic software package, and illustrations were drawn with ORTEP.

5. Supplementary material

Crystallographic data for the structural analysis have been deposited with the Cambridge Crystallographic Data Centre, CCDC Nos. 181587–181590 for the compounds **1**-C_s, **1**-C_1, **2**-C_s and **4**-C_s, respectively. Copies of this information may be obtained free of charge from The Director, CCDC, 12 Union Road, Cambridge CB2 1EZ, UK (Fax: +44-1223-336033; e-mail: deposit@ccdc.cam.ac.uk or www: http://www.ccdc.cam.ac.uk).

Acknowledgements

Y.T. is a research fellow of the Japan Society for the Promotion of Science, 2000–2002.

References

[1] (a) R. Alvarez, E. Carmona, J.M. Marïn, M.L. Poveda, E. Gutiërrez-Puebla, A. Monge, J. Am. Chem. Soc. 108 (1986) 2286;
(b) E.S. Marcos, R. Caballol, G. Trinquier, J.-C. Barthelat, J. Chem. Soc. Dalton Trans. (1987) 2373.

[2] Li-S. Wang, J.C. Fettinger, R. Poli, J. Am. Chem. Soc. 119 (1997) 4453.

[3] D.M. Schuster, J.L. Templeton, Organometallics 17 (1998) 2707.

[4] N.M. Agh-Atabay, J.L. Davidson, J. Chem. Soc. Dalton Trans. (1989) 1027.

[5] G.M. Gray, C.H. Duffey, Organometallics 13 (1994) 1542.

[6] O.P. Siclovan, R.J. Angelici, Inorg. Chem. 37 (1998) 432.

[7] (a) Y. Nakayama, H. Saito, N. Ueyama, A. Nakamura, Organometallics 18 (1999) 3149;
(b) Y. Takashima, Y. Nakayama, H. Yasuda, A. Nakamura, A. Harada, J. Organomt. Chem. 654 (2001) 74.

[8] (a) B.C. Ward, J.L. Templeton, J. Am. Chem. Soc. 102 (1980) 1532;
(b) J.L. Templeton, B.C. Ward, J. Am. Chem. Soc. 102 (1980) 3288;
(c) J.L. Templeton, B.C. Ward, G.-G.J. Chen, J.W. McDonald, W.E. Newton, Inorg. Chem. 20 (1981) 1248;
(d) J.L. Templeton, B.C. Ward, J. Am. Chem. Soc. 102 (1980) 3288;
(e) J.R. Morrow, T.L. Tonker, J.L. Templeton, Organometallics 4 (1985) 745;
(f) J.R. Morrow, T.L. Tonker, J.L. Templeton, J. Am. Chem. Soc. 107 (1985) 6956;
(g) J.L. Templeton, Adv. Organomet. Chem. 29 (1989) 1.

[9] S. Otsuka, A. Nakamura, Adv. Organomet. Chem. 14 (1976) 245.

[10] A. Mayr, K.S. Lee, M.A. Kjelsberg, D.V. Engen, J. Am. Chem. Soc. 109 (1986) 6079.

[11] L. Ricard, R. Weiss, W.E. Newton, G.J.-J. Chen, J.W. McDonald, J. Am. Chem. Soc. 100 (1978) 1318.

[12] (a) R.R. Schrock, L.W. Messerle, C.D. Wood, L.J. Guggenberger, J. Am. Chem. Soc. 100 (1978) 3793;
(b) R.R. Schrock, W.E. Crowe, G.C. Bazan, M. DiMare, M.B. O'Regan, M.H. Schofield, Organometallics 10 (1991) 1832.

[13] J. Kress, J.A. Osborn, J. Am. Chem. Soc. 109 (1987) 3953.

[14] For comprehensive reviews: (a) K.J. Ivin, J.C. Mol, Olefin Metathesis and Metathesis Polymerization, Academic Press, London, 1997;
(b) F.Z. Dörwald, Metal Carbenes in Organic Synthesis, Wiley-VCH, Weiheim, 1998;
(c) A. Fürstner, Alkene Metathesis in Organic Synthesis, Springer-Verlag, Berlin, 1998;
(d) R.R. Schrock, Pure Appl. Chem. 66 (1994) 1447.

[15] J. Feldman, R.R. Schrock, Prog. Inorg. Chem. 39 (1991) 1.

[16] R.R. Schrock, Acc. Chem. Res. 12 (1979) 98.

[17] R.H. Grubbs, W. Tumas, Science 243 (1989) 907.

[18] B.M. Novak, W. Risse, R.H. Grubbs, Adv. Polym. Sci. 102 (1990) 47.

[19] N.W. Eilerts, J.A. Heppert, Polyhedron 14 (1995) 3255.

[20] M. Schuster, S. Blechert, Angew. Chem. Int. Ed. Engl. 36 (1997) 2036.

[21] J.G. Hamilton, K.J. Ivin, J.J. Rooney, J. Mol. Catal. 28 (1985) 255.

[22] R.A. Andersen, G. Wilkinson, M.F. Lappert, R. Pearce, Inorg. Synth. 19 (1979) 262.

[23] T. Higashi, Program for Absorption Correction, Rigaku Corporation, Tokyo, Japan, 1995.

[24] G.M. Sheldrick, SHELXS-86, Program for the Solution of Crystal Structures, Universitat Göttingen, Germany, 1986.

[25] P.T. Beurskens, G. Admiraal, G. Beurskens, W.P. Bosman, R. de Gelder, R. Israel, J.M.M. Smits, The DIRDIF-94 Program System, Technical Report of the Crystallography Laboratory, University of Nijmegan, The Netherlands, 1994.

[26] G.M. Sheldrick, Program for the Solution of Crystal Structures, Universität Göttingen, Germany, 1997.

[27] A. Altomare, M.C. Burla, M. Camalli, M. Cascarano, C. Giacovazzo, A. Guagliardi, G. Polidori, J. Appl. Cryst. 27 (1994) 435.

[28] L.R. Gilliom, R.H. Grubbs, J. Am. Chem. Soc. 108 (1986) 733.

[29] N.A. Petasis, D.-K. Fu, J. Am. Chem. Soc. 115 (1993) 7208.